



Citation for published version:

Hamed Fasihnikoutalab, M, Pourakbar, S, Ball, R, Unuler, C & Cristelo, N 2020, 'Sustainable soil stabilisation with ground granulated blast-furnace slag activated by olivine and sodium hydroxide', *Acta Geotechnica*, vol. 15, pp. 1981-1991. <https://doi.org/10.1007/s11440-019-00884-w>

DOI:

[10.1007/s11440-019-00884-w](https://doi.org/10.1007/s11440-019-00884-w)

Publication date:

2020

Document Version

Peer reviewed version

[Link to publication](#)

This is a post-peer-review, pre-copyedit version of an article published in *Acta Geotechnica*. The final authenticated version is available online at: <https://doi.org/10.1007/s11440-019-00884-w>

University of Bath

Alternative formats

If you require this document in an alternative format, please contact:
openaccess@bath.ac.uk

General rights

Copyright and moral rights for the publications made accessible in the public portal are retained by the authors and/or other copyright owners and it is a condition of accessing publications that users recognise and abide by the legal requirements associated with these rights.

Take down policy

If you believe that this document breaches copyright please contact us providing details, and we will remove access to the work immediately and investigate your claim.

[Click here to view linked References](#)

1 November 2019 (R1)

2

3 **Sustainable soil stabilisation with ground**
4 **granulated blast furnace slag activated by**
5 **olivine and sodium hydroxide**

6

7 ^a Mohammad Hamed Fasihnikoutalab; ^b Shahram Pourakbar; ^c Richard J. Ball; ^d Cise Unluer;
8 ^{e,*} Nuno Cristelo

9

10 ^a Department of Civil Engineering, University Putra Malaysia, 43400 Serdang, Malaysia

11 Email address: hfasih@gmail.com

12

13 ^b PhD, Department of Civil Engineering, University of Binaloud, Mashhad, Iran

14 Email Address: pourakbar@binaloud.ac.ir

15

16 ^c BRE Centre for Innovative Construction Materials, Department of Architecture and Civil Engineering,
17 University of Bath, Bath, UK

18 Email Address: r.j.ball@bath.ac.uk

19

20 ^d School of Civil and Environmental Engineering, Nanyang Technological University, 639798 Singapore,
21 Singapore

22 Email address: ucise@ntu.edu.sg

23

24 ^e CQ-VR, Department of Engineering, University of Trás-os-Montes e Alto Douro, 5001-801 Vila Real,
25 Portugal

26 Email address: ncristel@utad.pt

27 Telephone: +351 259 350 000

28 * Corresponding author

50
51
52
53
54
55
56
57
58
59
60
61
62
63
64
65

29 **Abstract**

30

31 Ground granulated blast furnace slag (GGBS), activated with olivine (Mg_2SiO_4) and sodium
32 hydroxide (NaOH), was used to stabilise a clayey soil. Mechanical and microstructural
33 properties of the stabilised soil were assessed through uniaxial compression strength tests
34 (UCS), X-ray diffraction (XRD), scanning electron microscopy (SEM) and energy dispersive
35 X-ray spectroscopy (EDS), after curing periods of 7, 18 and 90 days. The UCS of the GGBS-
36 treated soil (without activation with NaOH), even at the highest slag dosage ($G_{20}S$), after 90
37 days, showed only a slight increase (142 kPa) relatively to the original soil. When olivine was
38 added to the GGBS-treated mixture ($O_{20}G_{20}S$), the UCS increased to 444 kPa, after 90 days.
39 However, when NaOH was used as an activator, the UCS of the olivine-GGBS treated soil
40 ($NO_{20}G_{20}S$) increased to more than 6000 kPa, after 90 days. This significant strength increase
41 was attributed to the higher reaction degree provided by the NaOH, which enabled a more
42 effective exploitation (dissolution) of the Ca and Mg present in the slag and olivine,
43 respectively, forming a mixture of C-S-H and M-S-H gels.

44

45 **Keywords:** Soil stabilisation; Alkaline activation; Olivine; Ground granulated blast furnace
46 slag

1. Introduction

Among the several ground improvement techniques now available, soil stabilisation with cement and lime is mostly and extensively used in road and railways, airport pavements, shallow foundations, embankments and deep soil stabilisation [1–5]. Although such traditional binders can improve many engineering properties of the original soils, they also possess several shortcomings, especially when viewed from an environmental perspective. In the case of Portland cement (OPC), its production requires high energy inputs and generates around 7% of anthropogenic CO₂ emissions [6]. It is estimated that every ton of cement produces nearly an equivalent amount of CO₂, a greenhouse gas that plays a major role in global warming [7, 8]. In addition to the CO₂ emissions, another by-product of cement production is NO_x. Indeed, a very significant volume of nitrogen oxides are produced in cement kilns, which can also contribute to the greenhouse effect and acid rain [9].

To reduce the environmental impacts associated with soil stabilisation, efforts are often focused on the development of new soil stabilisation methods that reduce the need for lime and, especially, cement. An interesting alternative are microbial biopolymers (i.e. excretions) capable of significant soil strengthening with as low as 10% of the equivalent cement content [10], or the better-known microbially induced carbonate precipitation technique, used to bind soil particles either for strength increase or pore filling [11]. This technique is already moving to the next evolution stage, as solutions for application of a single all-in-one shot are being successfully tested [12, 13]. Another popular route for developing new and environmentally friendly binders is based on industrial by-products and wastes, preferably those which are mostly constituted by amorphous aluminosilicates and exhibit pozzolanic properties. A wide variety of by-products was already successfully tested, including ground granulated blast furnace slag (GGBS), which proved to be a promising option for the replacement of traditional binders in soil stabilisation [14, 15]. Apart from the strong environmental benefit of reusing GGBS for soil stabilisation applications, there are also technical and economic reasons advantages [16, 17].

According to the study conducted by [18], a layer of Si–Al–O forms on the GGBS particle surfaces, when in contact with water. This layer can absorb H⁺ ions, resulting in an increase of OH⁻ ions as well as on the pH of the solution. However, this can be insufficient to efficiently break the Si–O and Al–O bonds, thus limiting the formation of calcium silicate

81 hydrate (CSH) and calcium aluminate hydrate (CAH) compounds. Therefore, the hydration
82 of GGBS can be enhanced via chemical activators. Most common activators used for this
83 purpose are lime (calcium oxide, CaO) and calcium hydroxide (Ca(OH)₂) [14]. Previous
84 applications of lime–GGBS mixtures in ground improvement included the treatment of
85 sulphate-bearing soils [19–21] and flooded low-capacity soils [22, 23].

86
87 Recent evidence suggests reactive magnesia (MgO) can also act as a sustainable GGBS
88 activator in ground improvement applications. Yi et al (2015) [24] investigated the use of
89 reactive magnesia (MgO) and carbide slag (CS) as sustainable activators for GGBS in clayey
90 soil stabilisation, concluding that the MgO-GGBS stabilised marine clay developed a
91 substantially higher 90-day compressive strength than the corresponding CS–GGBS
92 stabilised marine clay. Also, the 90-day UCS strength of MgO-GGBS stabilised soil doubled
93 the strength of the same soil stabilised with cement. In a different study, Yi et al (2014) [25]
94 compared the activating efficiency of a MgO-GGBS paste with a GGBS-hydrated lime paste,
95 and concluded that reactive MgO could act as an effective alkali activator of GGBS,
96 achieving higher 28-day strength than the corresponding GGBS-hydrated lime system.

97
98 Despite these findings, an important obstacle in the widespread application of MgO-GGBS in
99 soil stabilisation is related to environmental and economic issues. Given the fact that global
100 production of MgO is around 20 million tonnes per year, the price of the MgO that is suitable
101 for GGBS activation varies between 180\$ and 350\$ per ton [26]. Moreover, MgO is usually
102 produced by heating magnesium carbonate, which releases CO₂ into the atmosphere [27]. A
103 possible solution is the substitution of the MgO by olivine (Mg₂SiO₄), a magnesium silicate
104 mineral containing 45–49% of magnesium oxide (MgO) and 40% of silicon dioxide (SiO₂),
105 which can be considered a valid alternative source of MgO, to be used in soil improvement
106 [4, 5, 28, 29].

107
108 This study investigates the effectiveness of olivine (i.e. individually and in the presence of
109 NaOH) for GGBS activation, for soil stabilisation applications. To achieve this, the UCS test
110 was used as a practical indicator of strength development. The influence of GGBS and
111 olivine contents, as well as curing age, on the mechanical performance of stabilised soil
112 samples are discussed. These outcomes were further supported with microstructural analysis
113 to identify the mechanism responsible for strength development.

115

1
2 **116 2. Experimental Work**

3
4 117

5 *118 2.1 Materials*

6
7 119

8
9 120 The geotechnical properties and chemical composition of the clayey soil used in this
10
11 121 experiment are listed in Table 1 and Table 2, respectively. The soil was classified, according
12
13 122 to the Unified Soil Classification System [30], as a ‘high-plasticity clay’ (CH).

14
15 123

16 124 The chemical composition of the olivine mineral, obtained from Maha Chemicals Asia, is
17
18 125 also listed in in Table 2, showing MgO and SiO₂ contents of 48% and 40%, respectively. In
19
20 126 its original state, olivine had a significant volume of larger particles, thus requiring ball
21
22 127 milling, for 24 h at 60 rpm (around 65% of the critical speed), to decrease and homogenize
23
24 128 the particle size distribution, both presented in Figure 1. This approach was in line with the
25
26 129 pre-treatment process reported in earlier studies [4, 5] to increase the specific surface area
27
28 130 and, consequently, the reactivity of the olivine.

29 131

30
31 132

32
33 133

34
35 134

36
37 135

38
39 136

40
41 137

42
43 138

44
45 139

46
47 140 Figure 1: Particle size distribution of the olivine, after milling for 24h at 60 rpm

48
49 141

50
51 142 The GGBS, whose chemical composition is also listed in Table 2, was obtained from the
52
53 143 company *YTL Cement*. Sodium hydroxide (NaOH), supplied in pellets, was employed as an
54
55 144 alkali-activator after dissolution in distilled water, to a pre-designed concentration of 10 M.

56
57 145

58
59 146 Table 1: Geotechnical characteristics of the clayey soil

60
61 147

62
63 148

64
65

149

1
2 150 Table 2: Chemical composition of the soil, olivine and GGBS

3 151

4
5 152

6
7 153

8
9 154

10
11 155 *2.2 Specimen preparation and testing*

12 156

13
14 157 Table 3 presents the composition of the mixtures submitted to the UCS tests. Six distinct
15
16 158 groups were defined, each composed by different combinations, namely:

17
18 159

19
20 160 - Soil (S)

21 161 - Sodium hydroxide and soil (NS)

22 162 - GGBS and soil (GS)

23 163 - Olivine, GGBS and Soil (OGS)

24
25 164 - Sodium hydroxide, GGBS and soil (NGS)

26
27 165 - Sodium hydroxide, olivine, GGBS and soil (NOGS)

28
29 166

30
31 167 Table 3: Summary of the mixtures considered

32
33 168

34
35 169

36
37 170

38
39 171

40
41 172

42
43 173

44
45 174

46
47 175

48
49 176

50 177 The dry soil was initially mixed with the GGBS and, whenever necessary, with the olivine.

51
52 178 For the NGS and NOGS groups, the NaOH solution was added to the solids and thoroughly

53
54 179 mixed until a uniform blend was achieved. During this stage, additional water was added to

55
56 180 the mixture to meet the optimum moisture content of the stabilised samples.

57
58 181

59
60

61
62

63
64

65

182 Standard Proctor compaction tests were conducted for each mixture to obtain the moisture-
183 density relationship of the mixtures [31]. The maximum dry density (MDD) and optimum
184 water content (OWC) of each mixture are presented in Table 3.

185
186 Once mixing was completed, the specimens were manually compacted in cylindrical moulds
187 of 50 mm in diameter and 100 mm in height, using a 45 mm diameter steel rod to apply a
188 static load, in three layers. After compaction, the specimens were extruded and immediately
189 wrapped in plastic film and polythene covers to prevent moisture loss. The curing occurred at
190 room temperature (24°) for 7, 28, and 90 days. In order to achieve a state of near saturation,
191 thus avoiding any suction effects, the specimens were unwrapped and submerged in water for
192 the 24 h prior to the UCS test. The exception to this saturation procedure were the S and GS
193 groups, due to the loss of structural integrity of these samples when submerged.

194
195 The UCS test was conducted in accordance with [32]. An Instron 3366 universal testing
196 machine, fitted with a 100 kN load cell, was used for the test, which was carried out under
197 monotonic displacement control, at a rate of 0.2 mm/min. The entire stress-strain curve was
198 obtained for each test. Three different specimens were used for each data point.

199
200 The effect of the different activators and mix designs on sample development were further
201 investigated via energy dispersive X-ray spectroscopy (EDS), scanning electron microscopy
202 (SEM) and X-ray diffraction (XRD). Suitable samples for these analyses were extracted from
203 the UCS specimens, after testing. Specimens for SEM/EDS analysis were prepared by
204 crushing the treated soil specimens and then mounting them on Al-stubs with double-sided
205 carbon tapes prior to sputter coating with a thin layer of platinum. Analysis was performed on
206 a field emission scanning electron microscope (JSM 5700) coupled with an energy dispersive
207 X-ray spectrometer. XRD was performed on a Bruker D8 ADVANCE X-ray diffractometer,
208 with CuK_α radiation, at 40 kV and 40 mA emission current.

211 **3. Results**

213 *3.1 Mechanical performance*

215 The stress-strain behaviour of the olivine-GGBS treated soil, containing different percentages
216 of olivine and GGBS (OGS group), at curing periods of 7, 28 and 90 days, is shown in Figure
217 2. The stress-strain behaviour of the natural soil (S) and the GGBS-treated soil (GS group)
218 are also presented in these figures, for comparison purposes. The 7-day UCS values of the GS
219 group specimens improved slightly with the increase in GGBS content, which is most likely
220 related with a higher volume of calcium silicate hydrate (C-S-H) gel, resulting from the
221 soluble calcium present in the GGBS. The UCS of the mixtures that included olivine in its
222 composition (OGS group) achieved higher values than the corresponding mixtures without
223 olivine (GS group). The presence of olivine creates a source of partially dissolved MgO,
224 allowing the formation of a magnesium silicate hydrate (M-S-H) gel that coexists with the
225 main C-S-H gel.

227 Regarding the UCS evolution with curing time, presented in Figure 3, the data indicates that
228 an increase in GGBS content enhances the influence of curing time on compressive strength,
229 even if the short-term improvement is very similar for all three contents. This effect was also
230 observed for the O15GS and O20GS groups, although only for the 90-day curing period,
231 since the differences after 7 and 38 curing were practically neglectable. The 90-day UCS of
232 the GS and OGS groups was approximately 2x and 11x times higher than the UCS of the
233 natural soil (S), respectively. In short, these results indicate that, for longer curing periods (28
234 days and, especially, 90 days), the MgO potentiates the GGBS performance.

Figure 2: Stress-strain behaviour of the soil (S), the GGBS treated soil (G) and the olivine-GGBS treated soil (OG), after 7, 28 and 90 days curing

249

250

251

252

253

254

255

256

257

Figure 3: Influence of curing time on the UCS of the soil-stabiliser mixtures without sodium hydroxide

258

259

260

261

262

263

264

265

266

267

268

269

270

271

272

273

274

275

276

277

278

279

280

281

Figure 4 shows a comparative analysis of the stress-strain behaviour of the NaOH-GGBS-olivine treated soil (NOGS group), after 7, 28 and 90 days curing. The stress-strain curves of the natural soil (S), of the soil activated with NaOH (NS) and the NaOH-GGBS-treated soil (NGS group) were also included in these figures. The sodium hydroxide, as expected, didn't produce any effect on the original compressive strength of the soil, showing a very similar stress-strain path during the test, which didn't evolve with curing time. After 7 days curing, the UCS of the NGS mixtures slightly increased with higher GGBS contents, suggesting that the presence of GGBS in the NaOH solution formed an aluminum-substituted calcium silicate hydrate gel, commonly known as C-A-S-H gel. The existence of Al ions resulted in a higher degree of polymerization and, also, on more efficient crosslinking between the C-S-H chains. This finding is consistent with the work of [33], who found that the availability of Al ions results in the formation of stronger C-S-H chains. Further strength development was achieved by the addition of olivine to the mixture (NOGS group), reaching a maximum value of 6.1 MPa for the highest GGBS and olivine contents. The different UCS obtained by the NGS and NOGS groups was probably due to the higher amount of MgO dissolved by the NaOH.

The influence of the curing period on these pastes activated with sodium hydroxide is clearly lower than that shown for the no-NaOH pastes (Figure 5), even though the 90-day curing represented the highest UCS values, with the exception of the NO15G20S paste. Nevertheless, the curing period has to be considered a significant variable in the UCS of these pastes, since an increase between 20% and 100% was obtained when the curing period was extended between 7 and 90 days.

282

1
2 283

3
4 284

5
6 285

7
8 286

9
10 287

11
12 288

13
14 289

15
16 290

17 Figure 4: Stress-strain behaviour of the soil (S), the NaOH treated soil (NS), the NaOH-GGBS treated soil (NG)
18 and the NaOH-olivine-GGBS treated soil (NOG), after 7, 28 and 90 days curing

19
20 293

21
22 294

23
24 295

25
26 296

27
28 297

29
30 298

31
32 299

33
34 300

35
36 301

37
38 302

39 Figure 5: Influence of curing time on the UCS of the soil-stabiliser mixtures with sodium hydroxide

40
41 303

42
43 304

44
45 305

3.2 Microstructural analysis

46
47 306

48
49 307

SEM images of the olivine-GGBS treated soil ($O_{20}G_{20}S$ and $NO_{20}G_{20}S$ mixtures), after 90 days curing, are presented in Figure 6. The microstructure reveals the formation of a binding gel, resulting from the reactions between the olivine and GGBS precursors and the water or alkaline activator, connecting the unreacted olivine and GGBS particles and the clay particles. However, the use of water alone showed less dense formations (Figure 6a) than those obtained with an alkaline activator (Figure 6b), suggesting that the resulting gel and the subsequent crystallisation, produced by the latter, were more effective at occupying the initial voids of the soil, generating a more compact microstructure. This is probably a consequence of a higher dissolution rate of the amorphous species present in the olivine and GGBS [34].

50
51 308

52
53 309

54
55 310

56
57 311

58
59 312

60
61 313

62
63 314

64
65 315

316 This also explains the higher UCS values obtained by the mixture $\text{NO}_{20}\text{G}_{20}\text{S}$, as shown earlier
1 317 in Figure 6.
2

3 318

4 319

5 320

6 321

7 322

8 323

9 324

10 325

11 326

12 327

13 328

14 329

15 330

16 331

17 332

18 333

Figure 6: SEM images of mixtures $\text{O}_{20}\text{G}_{20}\text{S}$ (a) and $\text{NO}_{20}\text{G}_{20}\text{S}$ (b), after 90 days curing

19 334

20 335 The EDX data obtained from mixtures $\text{O}_{20}\text{G}_{20}\text{S}$ and $\text{NO}_{20}\text{G}_{20}\text{S}$, also shown in Figure 6 (only
21 336 two points per image, out of six, are presented) allowed the comparison between the
22 337 composition of the gels developed with and without NaOH. Ideally, this elemental analysis
23 338 would have been made using back-scattering, guaranteeing enhanced reliability and
24 339 precision. Since such option wasn't available, the spectra obtained can still be used to detect
25 340 gel areas, by comparison. This semi-quantitative elemental analysis (Na, Si, Al, Ca and Mg)
26 341 was used in the calculation of the Na/Al, Si/Al, Ca/Al, Mg/Si and Ca/Si atomic ratios,
27 342 presented in Table 4.
28 343

29 344

30 345 Differences in the nature of the gel are easily identifiable between the mixture fabricated with
31 346 a highly alkaline activator and the mixture fabricated with water. With the addition of NaOH,
32 347 the Si/Al ratio increased, as a result of a more effective capacity, shown by the NaOH-based
33 348 mixture, to dissolve the Si present in the olivine and GGBS (both precursors had originally a
34 349 significantly lower content in Al than Si). However, and according to Provis (2014) [35], the
35 350 soil particles could also have reacted with the alkaline solution, thus contributing to the Si

350 released into the ion ‘soup’ that later resulted in the binding gel. The Mg/Si and Ca/Si ratios
351 also increased with the inclusion of sodium hydroxide in the mixture (from 0.031 to 0.063
352 and 0.124 to 0.133, respectively), suggesting that the Ca from the GGBS and the Mg from the
353 olivine were also more effectively dissolved with the NaOH, favouring the development of a
354 combination of C-S-H and M-S-H gels. The idea that the dissolution of Al was hindered by
355 the presence of NaOH, comparing with the remaining species, is reinforced by the fact that
356 the increase in the Mg/Al and Ca/Al ratios, from OGS to NOGS mixtures (from 0.046 to
357 0.162 and 0.182 to 0.291, respectively), was significantly higher than the corresponding
358 Mg/Si and Ca/Si increases.

Table 4: Average atomic ratios for mixtures $O_{20}G_{20}S$ and $NO_{20}G_{20}S$, after 90 days curing

361
362
363
364
365
366
367 The crystalline phases formed in mixtures $O_{20}G_{20}S$ and $NO_{20}G_{20}S$, as determined by XRD
368 analysis, are shown in Figure 7. The main phases observed in the $O_{20}G_{20}S$ sample were
369 quartz, kaolinite, magnesium and magnesium oxide, while calcium oxide and calcium silicate
370 hydrate were also detected. All these are common phases in olivine-GGBS stabilised clayey
371 soils, with intensities varying only with the type of clay mineral. The same main phases were
372 observed in the $NO_{20}G_{20}S$ mixture, although part of the kaolinite phase appears to have been
373 dissolved in the reactions promoted by the alkaline activator. The XRD data supported the
374 presence of gel-like or reticular C-S-H fume in sample $O_{20}G_{20}S$, as a result of the hydration
375 process, which is in line with the findings reported by [5, 27, 36]. The intensity of the
376 magnesium-based peaks is lower in the $NO_{20}G_{20}S$ mixture, revealing that the olivine is more
377 effectively incorporated with NaOH than water. Haha et al (2011) [37] demonstrated that
378 increasing the MgO content in MgO-GGBS mixtures resulted in a higher volume of
379 hydration products and higher strength development in slag pastes activated by NaOH.
380 Therefore, these findings could explain the high strength developed in OGS and NOGS
381 groups presented in Figures 2 to 7.

383

1
2 384

3
4 385

5
6 386

7
8 387

9
10 388

11
12 389

13
14 390

15
16 391

Figure 7: XRD diffractograms of mixtures O20G20S and NO20G20S, after 90 days curing (legend: q - quartz; c - calcium silicate hydrate; k - kaolinite; mg - magnesium; mgo - magnesium oxide; m - mullite; cao - calcium oxide)

17
18 393

19
20 394

21
22 395

23
24 396

4. Discussion

25
26 397

27
28 398

The UCS as a function of the stabiliser/solids ratio, after 7, 28 and 90 days, is presented in Figure 8. The terms ‘stabiliser’ and ‘solids’ were defined as the sum of components of the stabiliser, in dry form (GGBS + Olivine), and as the sum of these components with the soil (Soil + GGBS + Olivine), respectively.

29
30 400

31
32 401

33
34 402

35
36 403

Both the OGS group (without NaOH) and the NOGS group (with NaOH) are represented. Two observations can easily be drawn: an increase in curing time (up to 90 days) yielded higher compressive strength; and an increase in the stabiliser content was also highly beneficial for strength development. This second observation was particularly valid for the mixtures activated with sodium hydroxide, which showed R-squared values not lower than 95%. The strength gain rate of these mixtures was also superior to that of the OGS mixtures, further highlighting the role of the alkaline activator. The R-squared value for the 90-day curing of the mixtures without NaOH was relatively low (64%), mostly due to the UCS values registered by the mixtures prepared with a stabiliser/solids ratio of 0.35, which are clearly lower than the 0.30 and 0.40 UCS values. This is a possible consequence of the fact that such mixtures were prepared with the lowest olivine / GGBS ratio (0.75) of the whole experimental campaign.

37
38 404

39
40 405

41
42 406

43
44 407

45
46 408

47
48 409

49
50 410

51
52 411

53
54 412

55
56 413

57
58 414

59
60 415

61
62

63
64

65

416
1
2 417
3
4 418
5 419
6
7 420
8
9 421
10
11 422
12
13 423
14 424
15
16 425
17
18 426
19
20 427
21 428
22
23 429
24
25 430
26
27 431
28
29 432
30
31 433
32
33 434
34
35 435
36
37 436
38
39 437
40
41 438
42
43 439
44
45 440
46
47 441
48
49 442
50
51
52
53
54
55
56
57
58
59
60
61
62
63
64
65

Figure 8: UCS evolution of the OGS and NOGS groups as a function of the stabiliser/solids ratio, at different curing times (the terms ‘Stabiliser’ and ‘Solids’ were defined as the ‘GGBS+Olivine’ dry sum and ‘Soil+GGBS+Olivine’ dry sum, respectively)

The highest UCS values obtained by the 15%-olivine mixtures (either in the OGS and NOGS groups), after 90 days, were inferior to the lowest UCS obtained by the 20%-olivine mixtures. However, the latter group also had a higher stabiliser/solids content than the former. In order to better assess the effect of the olivine on the quality of the mixtures, the UCS values obtained with mixtures with the same stabiliser/solids content (0.20 or 0.25) were compared in Figure 9. The positive influence of the MgO is especially clear with the increase from 0% to 15%, and especially when sodium hydroxide was used. Note that this increase in olivine represented a decrease of the GGBS content, from 20% to 5%, suggesting that the MgO plays a more relevant role than the Ca from the slag. The reason behind the favourable effect of the olivine in the overall mechanical strength of the mixtures is probably related with the capacity of the MgO to reduce porosity [24]. Nonetheless, the increase in olivine from 15% to 20% didn’t produce such a positive effect, indicating there is an optimum ratio olivine/GGBS.

444

1
2 445

3
4 446

5
6 447

7
8 448

9
10 449

11 450

12
13 451

14
15 452

16
17 453

18
19 454

20
21 455

22
23 456

24
25 457

26
27 458

28
29 459

30
31 460

32
33 461

34
35 462

36
37 463

38
39 464

40
41 465

42
43 466

44
45 467

46
47 468

48
49 469

50
51 470

52
53 471

54
55 472

56
57 473

58
59 474

60
61 475

62
63 476

64
65 477

Figure 9: UCS evolution with curing time and olivine content for two different stabiliser / solids ratios (0.20 and 0.25)

Other authors, studying the stabilisation of a marine soft clay with GGBS activated by carbide slag [16], found a maximum UCS value of 3.8 MPa (after 28 days) for a carbide/GGBS ratio of 0.15, after which the UCS steadily decreased, reaching a value of 2.5 MPa for a 0.40 ratio. These values were obtained for a GGBS/soil ratio of 0.30. When the GGBS/soil ratio decreased to 0.20, the peak UCS, after 28 days, decreased also to 2.8 MPa, obtained with a carbide/GGBS ratio of 0.25. During the present research, similar GGBS/soil ratios were used (values of 0.053, 0.111 and 0.250), although with very different activator / GGBS ratios (the activator, in this case, was olivine), ranging from 0.75 to 4.0. Nonetheless, the results are comparable and consistent with those presented by other authors, since the UCS, after 28 days, start at approximately 0.4 MPa and 0.5 MPa, for olivine/GGBS ratios of 0.75 and 1.0, respectively. These values are in line with the findings of the research mentioned above, assuming that the UCS values would continue to decrease with the increase in the activator/GGBS ratio.

A similar study, from the same authors, tested the effectiveness of lime to act as the GGBS activator [38]. The results showed a similar trend, i.e. the existence of an optimum activator/GGBS dry weight ratio, although, in this case, lower UCS values were obtained:

478 approximately 1.8 MPa and 1.6 MPa, for quicklime and hydrated lime, respectively, both
479 with an activator/GGBS ratio of 0.20 and a GGBS/soil ratio of 0.20.

480
481 Yi et al, in 2014 [39], also studied the effect of binders made from GGBS activated either
482 with lime or MgO on the stabilisation of two soils. The results are in accordance with those
483 presented above. The MgO-based UCS results were, once again, far superior to the lime-
484 based results, and the activator (MgO or lime) / GGBS ratio proved also to have an optimum
485 value which, in this case, was again 0.20. Further increase of this ratio was detrimental to the
486 UCS development, even if the binder contents tested are significantly lower (only up to 0.10)
487 than the ones used in the current study.

488
489 Based on the results and subsequent discussion and comparison with similar studies, it is
490 possible to assume that the increase in stabiliser content improves the mechanical behaviour
491 of the soil, that the inclusion of olivine has a positive effect on the formation of hydration gel,
492 but also that such olivine content has an optimum value to potentiate the quality of the
493 binding gel formed.

496 5. Conclusions

497
498 The present study focused on the use of olivine, as a reliable and sustainable source of MgO,
499 to enhance the effectiveness of alkali activated ground granulated blast furnace slag. The
500 resulting binder was applied to the stabilisation of a clayey soil, which was then assessed
501 through uniaxial compression strength tests, X-ray diffraction, scanning electron microscopy
502 and energy dispersive X-ray spectroscopy, after curing periods of 7, 18 and 90 days. The
503 following conclusion were drawn:

- 504
505 - The high alkalinity of the NaOH promoted a more effective dissolution of the olivine
506 and GGBS precursors, leading also to higher strength development of the stabilised
507 soil mixtures, compared with the water-based mixtures.
- 508 - UCS results demonstrated that the addition of olivine to the GGBS-soil combinations
509 improved strength development, as demonstrated by the UCS values obtained with
510 15% and 20% olivine.

- 511 - The olivine/GGBS ratio should be optimised, as an increase in such ratio produces a
 1 strength decrease, for all curing periods, but only up to a certain level.
 2 512
 3
 4 513 - There was a clear strength increase with curing time, at least until 90 days, regardless
 5 of the composition considered.
 6 514
 7 515 - The UCS clearly increased with the stabiliser/solids wt. ratio. Since this ratio increase
 8 represented also a decrease of the olivine/GGBS wt. ratio, it was necessary to
 9 516 establish which of these two factors was responsible for the strength increase.
 10 517
 11 518 - A combination of C-S-H gel and M-S-H gel was observed in the SEM/EDS analysis,
 12 as a result of the addition of olivine (MgO) to the GGBS (CaO) precursor.
 13 519
 14
 15
 16 520
 17
 18 521

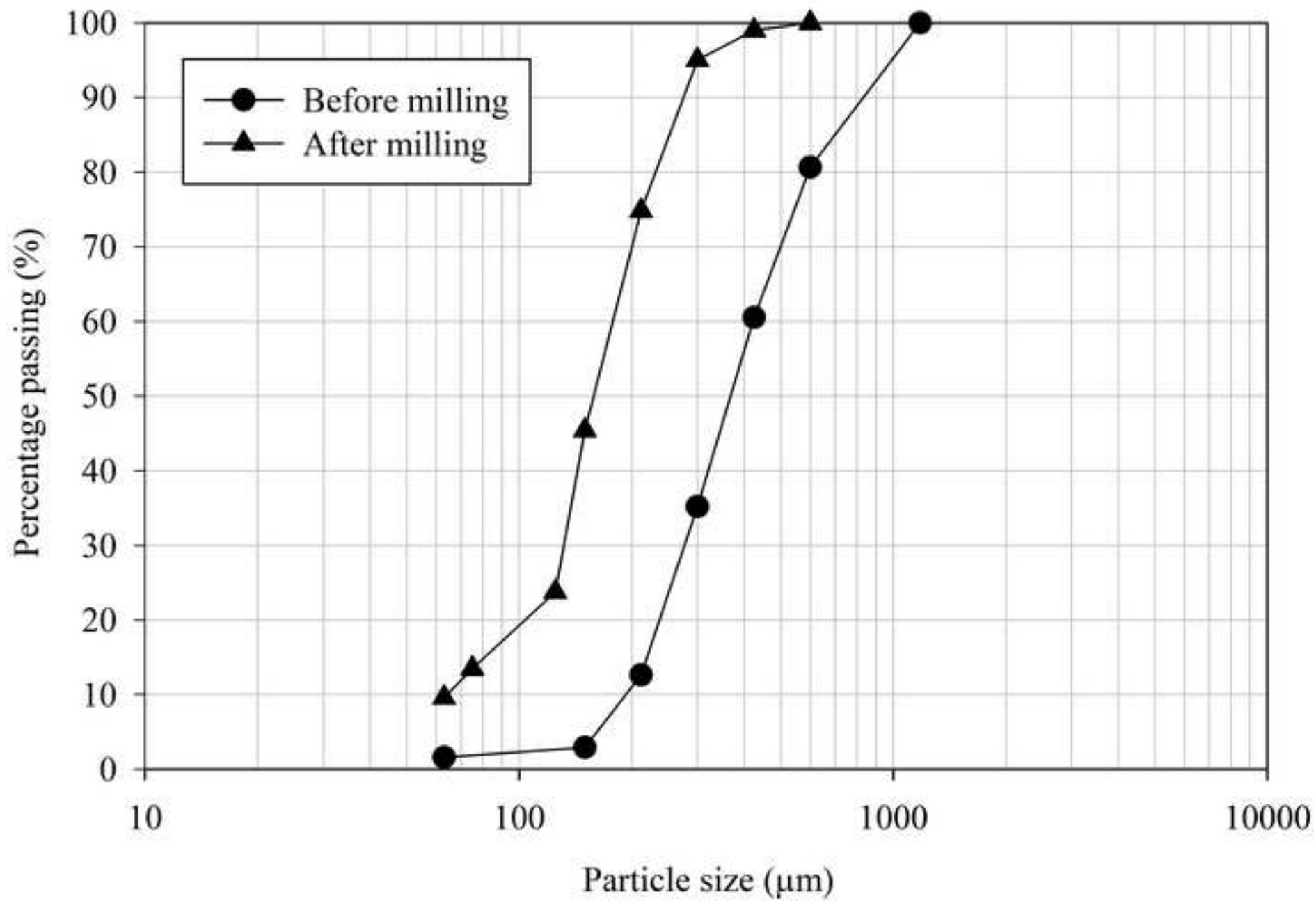
20 522 **References**

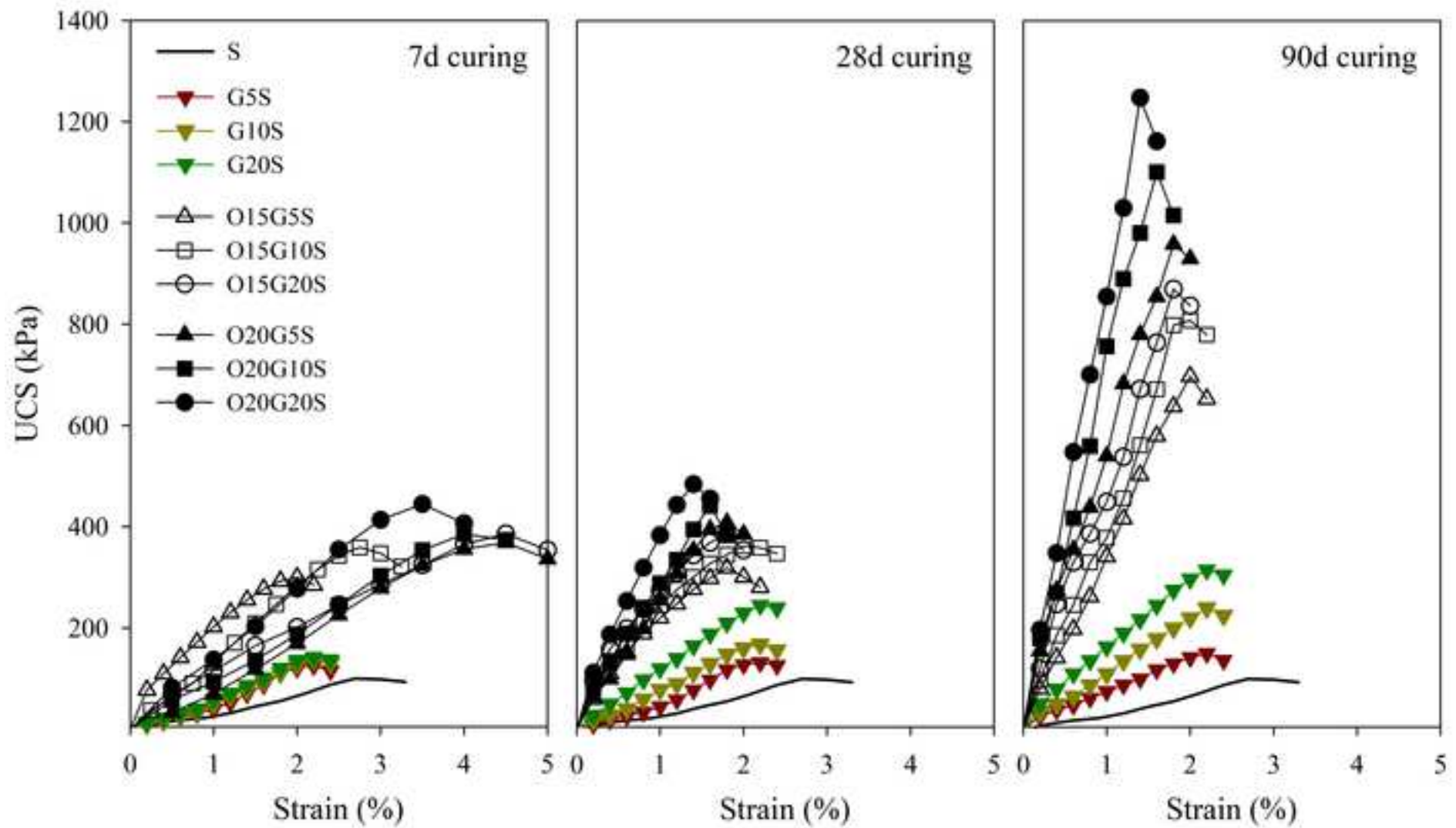
- 21 523
 22
 23 524 1. Horpibulsuk S, Bergado DT, Lorenzo GA (2004) Compressibility of cement-admixed
 24 clays at high water content. *Géotechnique* 54:151–154 . doi:
 25 10.1680/geot.54.2.151.36341
 26 525
 27 526
 28 527 2. Horpibulsuk S, Miura N, Nagaraj TS (2004) Assessment of strength development in
 29 cement-admixed high water content clays with Abrams’ law as a basis. *Géotechnique*
 30 528 53:439–444 . doi: 10.1680/geot.53.4.439.37319
 31 529
 32 530 3. Porbaha A (1998) State of the art in deep mixing technology: part I. Basic concepts
 33 and overview. *Proc Inst Civ Eng - Gr Improv* 2:81–92 . doi: 10.1680/gi.1998.020204
 34 531
 35 532 4. Pourakbar S, Asadi A, Huat BBK, Fasihnikoutalab MH (2015) Stabilization of clayey
 36 soil using ultrafine palm oil fuel ash (POFA) and cement. *Transp Geotech* 3:24–35 .
 37 533 doi: 10.1016/j.trgeo.2015.01.002
 38 534
 39 535 5. Ball RJ, Pourakbar S, Huat BK, et al (2016) Utilisation of carbonating olivine for
 40 sustainable soil stabilisation. *Environ Geotech* 4:184–198 . doi:
 41 10.1680/jenge.15.00018
 42 536
 43 537
 44 538 6. Gartner E (2004) Industrially interesting approaches to “low-CO₂” cements. *Cem*
 45 *Concr Res* 34:1489–1498 . doi: 10.1016/j.cemconres.2004.01.021
 46 539
 47 540 7. Kim Y, Worrell E (2002) CO₂ emission trends in the cement industry: An
 48 international comparison. *Mitig Adapt Strateg Glob Chang* 7:115–133 . doi:
 49 10.1023/A:1022857829028
 50 541
 51 542
 52 543 8. Lothenbach B, Scrivener K, Hooton RD (2011) Supplementary cementitious materials.
 53 *Cem Concr Res* 41:1244–1256 . doi: 10.1016/j.cemconres.2010.12.001
 54 544
 55
 56
 57
 58
 59
 60
 61
 62
 63
 64
 65

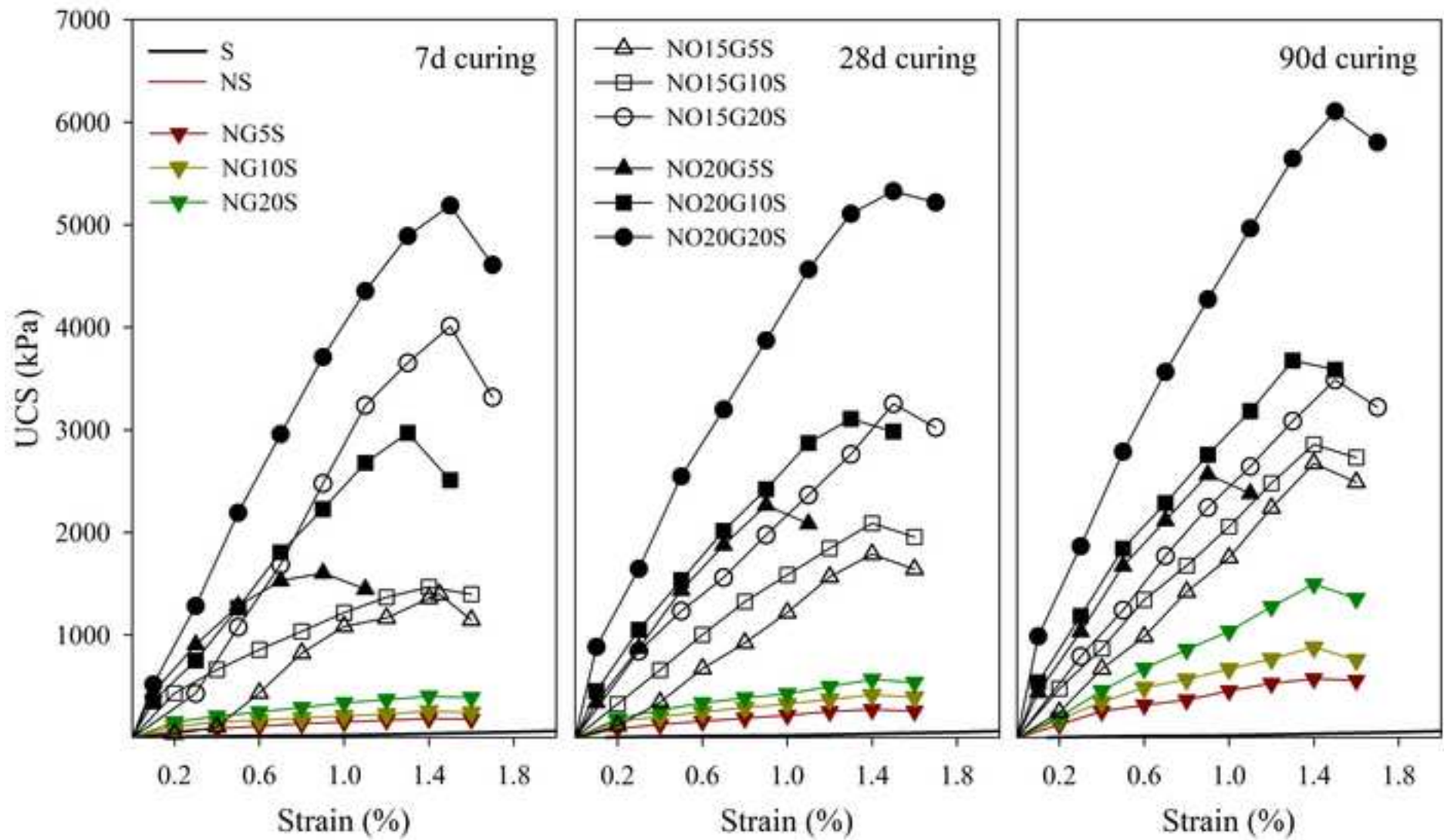
- 545 9. Riemer P, Hendriks C, Ozawa Meida L, et al (2007) Emission reduction of greenhouse
1 546 gases from the cement industry. In: *Greenhouse Gas Control Technologies 4*. pp 939–
2 547 944
- 3 548 10. Chang I, Cho GC (2019) Shear strength behavior and parameters of microbial gellan
4 549 gum-treated soils: from sand to clay. *Acta Geotech* 14:361–375
- 5 550 11. Wu C, Chu J, Wu S, et al (2019) Microbially induced calcite precipitation along a
6 551 circular flow channel under a constant flow condition. *Acta Geotech* 14:673–683
- 7 552 12. Cheng L, Shahin MA, Chu J (2019) Soil bio-cementation using a new one-phase low-
8 553 pH injection method. *Acta Geotech* 14:615–626
- 9 554 13. Wang X, Tao J (2019) Polymer-modified microbially induced carbonate precipitation
10 555 for one-shot targeted and localized soil improvement. *Acta Geotech* 14:657–671
- 11 556 14. Nidzam RM, Kinuthia JM (2010) Sustainable soil stabilisation with blastfurnace slag –
12 557 a review. *Proc Inst Civ Eng - Constr Mater* 163:157–165 . doi:
13 558 10.1680/coma.2010.163.3.157
- 14 559 15. Du YJ, Wu J, Bo YL, Jiang NJ (2019) Effects of acid rain on physical, mechanical and
15 560 chemical properties of GGBS–MgO-solidified/stabilized Pb-contaminated clayey soil.
16 561 *Acta Geotech*. doi: <https://doi.org/10.1007/s11440-019-00793-y>
- 17 562 16. Yi Y, Gu L, Liu S, Puppala AJ (2015) Carbide slag-activated ground granulated
18 563 blastfurnace slag for soft clay stabilization. *Can Geotech J* 52:656–663
- 19 564 17. Jegandan S, Liska M, Osman AA-M, Al-Tabbaa A (2010) Sustainable binders for soil
20 565 stabilisation. *Proc Inst Civ Eng - Gr Improv* 163:53–61 . doi:
21 566 10.1680/grim.2010.163.1.53
- 22 567 18. Shi C, Day RL (1993) Chemical activation of blended cements made with lime and
23 568 natural pozzolans. *Cem Concr Res* 23:1389–1396 . doi: 10.1016/0008-8846(93)90076-
24 569 L
- 25 570 19. Higgins DD, J M Kinuthia JM, Wild S (1998) Soil Stabilization using Lime-Activated
26 571 Ground Granulated Blast Furnace Slag. *Spec Publ* 178:1057–1074 . doi:
27 572 10.14359/6023
- 28 573 20. Wild S, Kinuthia JM, Jones GI, Higgins DD (1998) Effects of partial substitution of
29 574 lime with ground granulated blast furnace slag (GGBS) on the strength properties of
30 575 lime-stabilised sulphate-bearing clay soils. *Eng Geol* 51:37–53 . doi: 10.1016/S0013-
31 576 7952(98)00039-8
- 32 577 21. Wild S, Kinuthia JM, Robinson RB, Humphreys I (2006) Effects of ground granulated
33 578 blast furnace slag (GGBS) on the strength and swelling properties of lime-stabilized

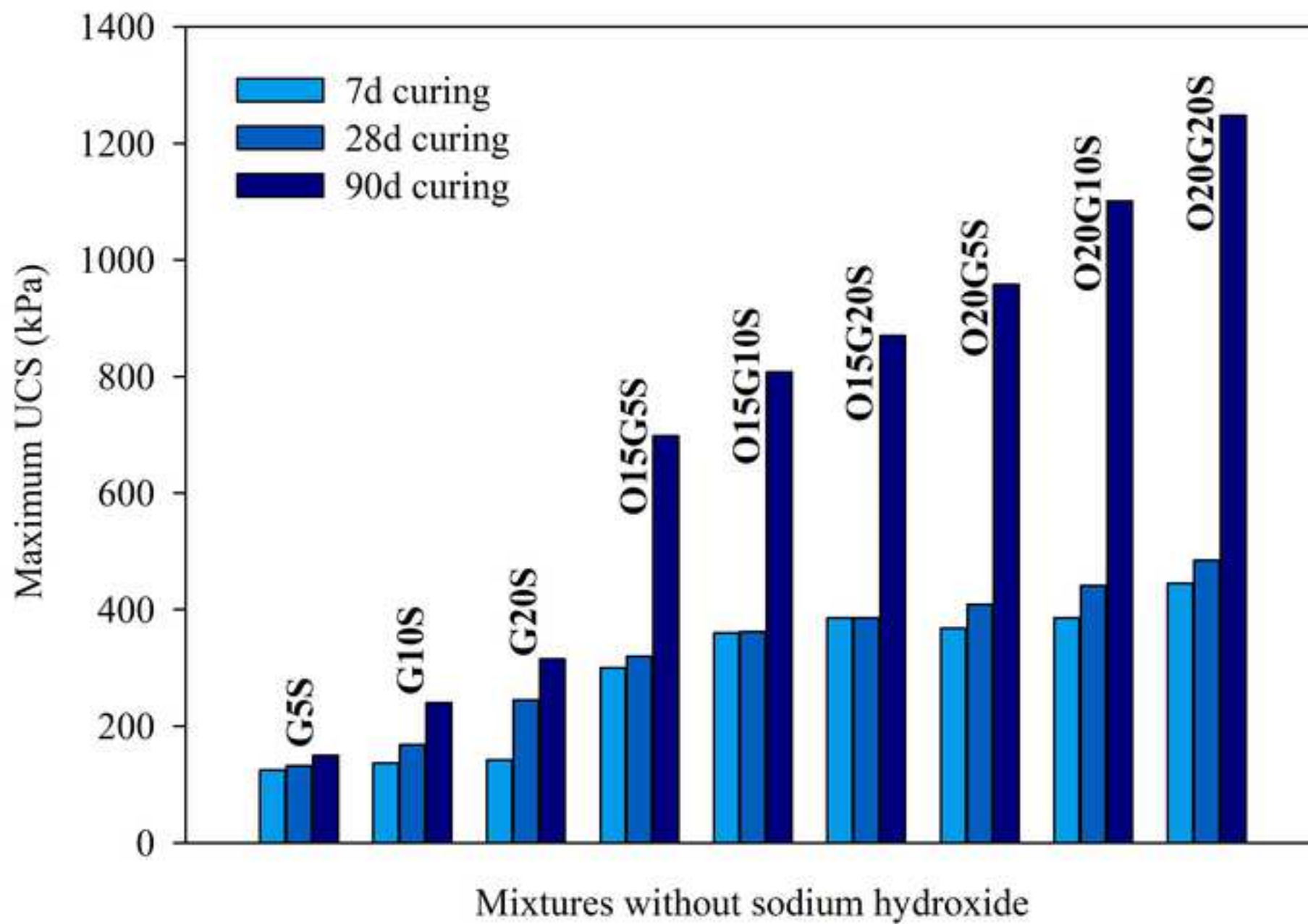
- 579 kaolinite in the presence of sulphates. *Clay Miner* 31:423–433 . doi:
1 580 10.1180/claymin.1996.031.3.12
2
3 581 22. Obuzor GN, Kinuthia JM, Robinson RB (2011) Enhancing the durability of flooded
4
5 582 low-capacity soils by utilizing lime-activated ground granulated blastfurnace slag
6
7 583 (GGBS). *Eng Geol* 123:179–186 . doi: 10.1016/j.enggeo.2011.07.009
8
9 584 23. Obuzor GN, Kinuthia JM, Robinson RB (2012) Soil stabilisation with lime-activated-
10
11 585 GGBS-A mitigation to flooding effects on road structural layers/embankments
12
13 586 constructed on floodplains. *Eng Geol* 151:112–119 . doi:
14
15 587 10.1016/j.enggeo.2012.09.010
16
17 588 24. Yi Y, Zheng X, Liu S, Al-Tabbaa A (2015) Comparison of reactive magnesia- and
18
19 589 carbide slag-activated ground granulated blastfurnace slag and Portland cement for
20
21 590 stabilisation of a natural soil. *Appl Clay Sci* 111:21–26 . doi:
22
23 591 10.1016/j.clay.2015.03.023
24
25 592 25. YI Y, LI C, LIU S, AL-TABBAA A (2014) Resistance of MgO–GGBS and CS–
26
27 593 GGBS stabilised marine soft clays to sodium sulfate attack. *Géotechnique* 64:673–679
28
29 594 . doi: 10.1680/geot.14.t.012
30
31 595 26. Al-Tabbaa A, Liu C, Gao L, et al (2015) Incorporation of reactive magnesia and
32
33 596 quicklime in sustainable binders for soil stabilisation. *Eng Geol* 195:53–62 . doi:
34
35 597 10.1016/j.enggeo.2015.05.025
36
37 598 27. Fasihnikoutalab MH, Asadi A, Kim Huat B, et al (2016) Laboratory-scale model of
38
39 599 carbon dioxide deposition for soil stabilisation. *J Rock Mech Geotech Eng* 8:178–186 .
40
41 600 doi: 10.1016/j.jrmge.2015.11.001
42
43 601 28. Huat BK, Ball RJ, Asadi A, et al (2017) Utilization of Alkali-Activated Olivine in Soil
44
45 602 Stabilization and the Effect of Carbonation on Unconfined Compressive Strength and
46
47 603 Microstructure. *J Mater Civ Eng* 29:06017002 . doi: 10.1061/(asce)mt.1943-
48
49 604 5533.0001833
50
51 605 29. Fasihnikoutalab MH, Pourakbar S, Ball RJ, Huat BK (2017) The Effect of Olivine
52
53 606 Content and Curing Time on the Strength of Treated Soil in Presence of Potassium
54
55 607 Hydroxide. *Int J Geosynth Gr Eng* 3:12 . doi: 10.1007/s40891-017-0089-3
56
57 608 30. ASTM D2487-11 (2011) Standard Practice for Classification of Soils for Engineering
58
59 609 Purposes (Unified Soil Classification System). Am Soc Test Mater
60
61 610 31. BSi 1377-4 (1990) BS 1377-4: 1990 - Methods of test for soils for civil engineering
62
63 611 purposes, Part 4: Compaction-Related Tests. Br Stand Institution, London 4:
64
65 612 32. BSi 1377-7 (1990) BS 1377-7: 1990 - Methods of test for soils for civil engineering

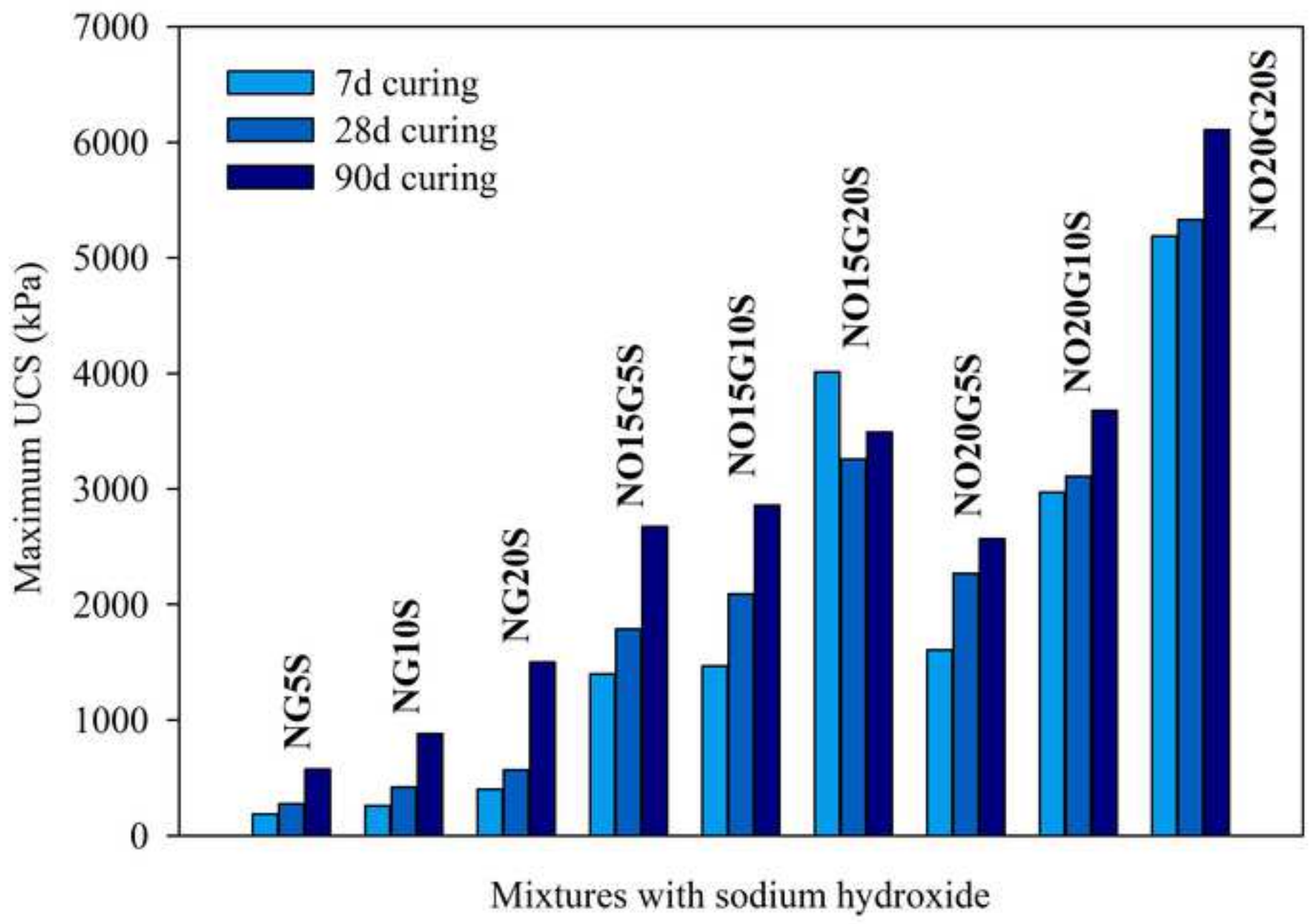
613 purposes, Part 7: Shear Strength Tests (Total Stress). Br Stand Institution, London 7:
 1 614 33. Richardson IG, Brough AR, Groves GW, Dobson CM (1994) The characterization of
 2 615 hardened alkali-activated blast-furnace slag pastes and the nature of the calcium
 3 616 silicate hydrate (C-S-H) phase. *Cem Concr Res* 24:813–829 . doi: 10.1016/0008-
 4 617 8846(94)90002-7
 5
 6 618 34. Yi Y, Liska M, Al-Tabbaa A (2013) Properties and microstructure of GGBS–magnesia
 7 619 pastes. *Adv Cem Res* 26:114–122 . doi: 10.1680/adcr.13.00005
 8
 9 620 35. Provis JL (2014) Geopolymers and other alkali activated materials: Why, how, and
 10 621 what? *Mater Struct Constr* 47:11–25
 11
 12 622 36. Konsta-Gdoutos MS, Shah SP (2003) Hydration and properties of novel blended
 13 623 cements based on cement kiln dust and blast furnace slag. *Cem Concr Res* 33:1269–
 14 624 1276 . doi: 10.1016/S0008-8846(03)00061-9
 15
 16 625 37. Haha M Ben, Lothenbach B, Le Saout G, Winnefeld F (2011) Influence of slag
 17 626 chemistry on the hydration of alkali-activated blast-furnace slag — Part I: Effect of
 18 627 MgO. *Cem Concr Res* 41:955–963 . doi: 10.1016/J.CEMCONRES.2011.05.002
 19
 20 628 38. Yi Y, Gu L, Liu S (2015) Microstructural and mechanical properties of marine soft
 21 629 clay stabilized by lime-activated ground granulated blastfurnace slag. *Appl Clay Sci*
 22 630 103:71–76
 23
 24 631 39. Yi Y, Liska M, Al-Tabbaa A (2014) Properties of two model soils stabilized with
 25 632 different blends and contents of GGBS, MgO, lime, and PC. *J Mater Civ Eng* 26:267–
 26 633 274
 27
 28
 29
 30
 31
 32
 33
 34
 35
 36
 37
 38
 39
 40
 41
 42
 43
 44
 45
 46
 47
 48
 49
 50
 51
 52
 53
 54
 55
 56
 57
 58
 59
 60
 61
 62
 63
 64
 65

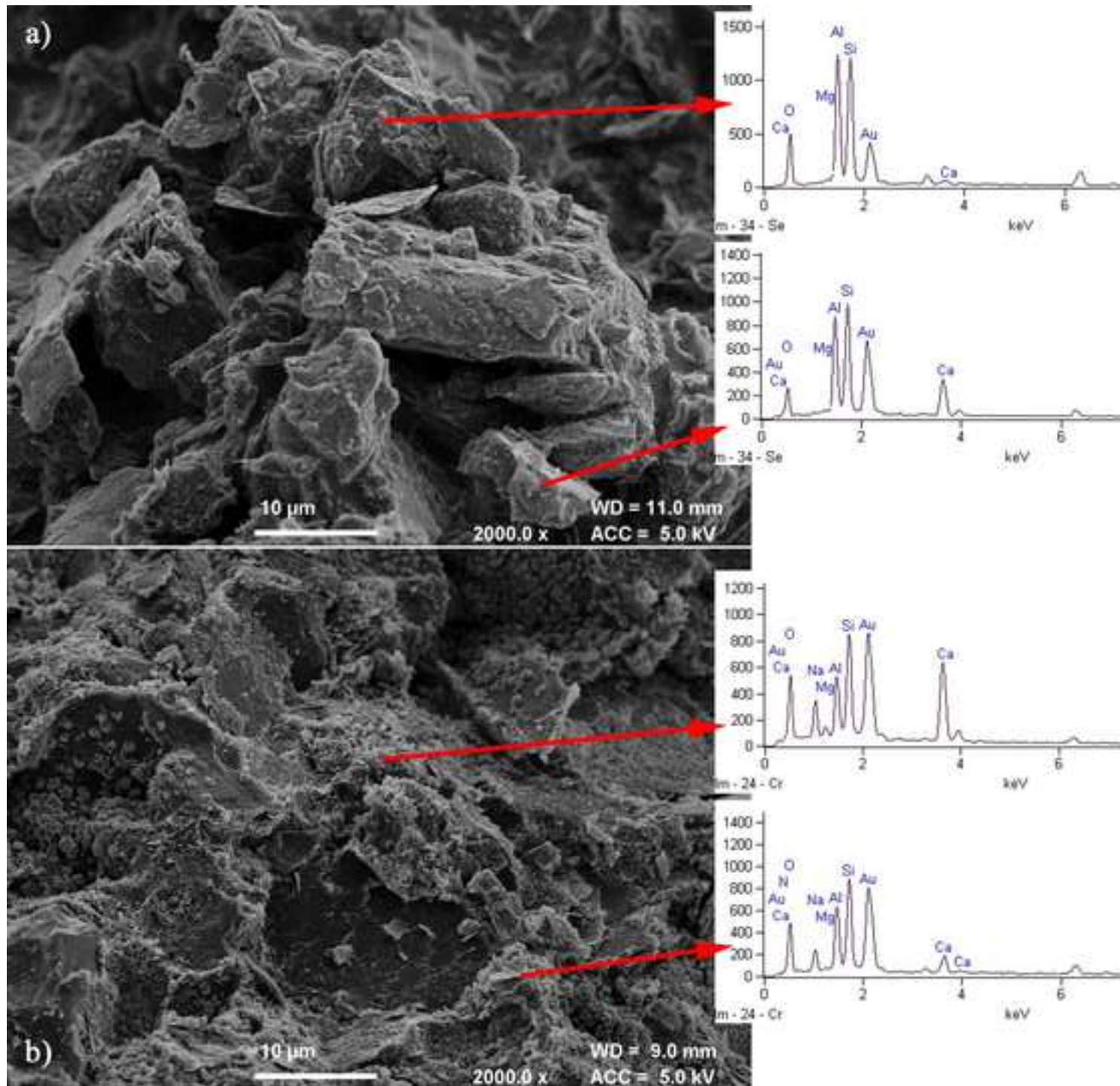


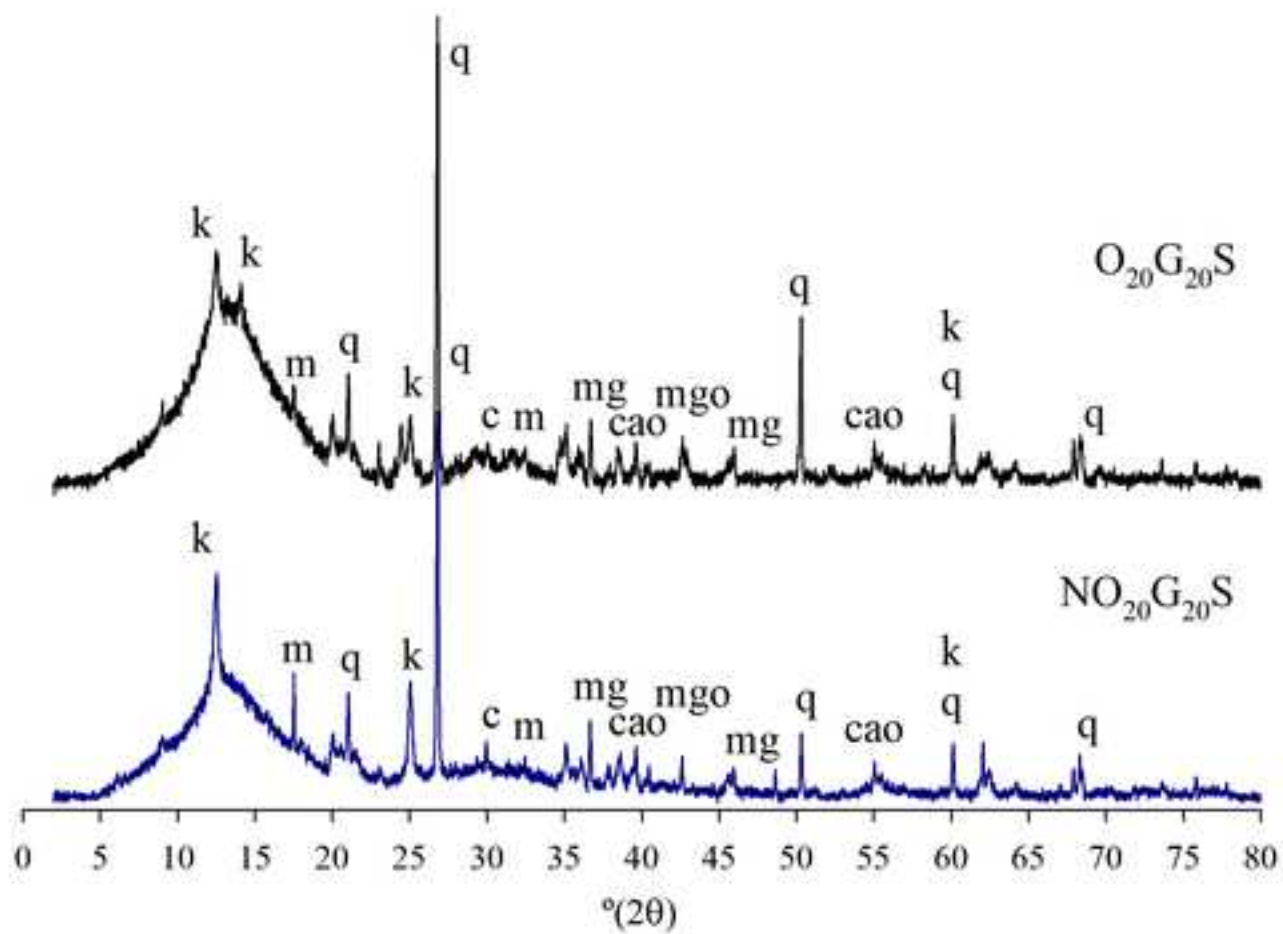


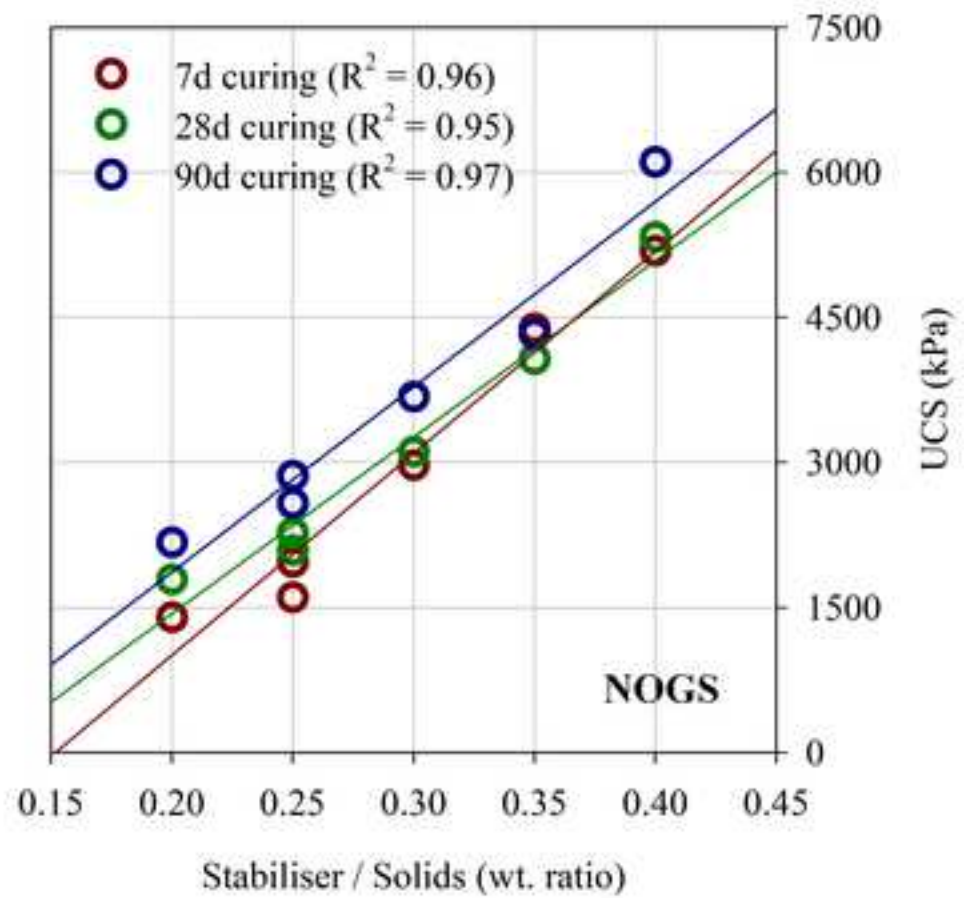
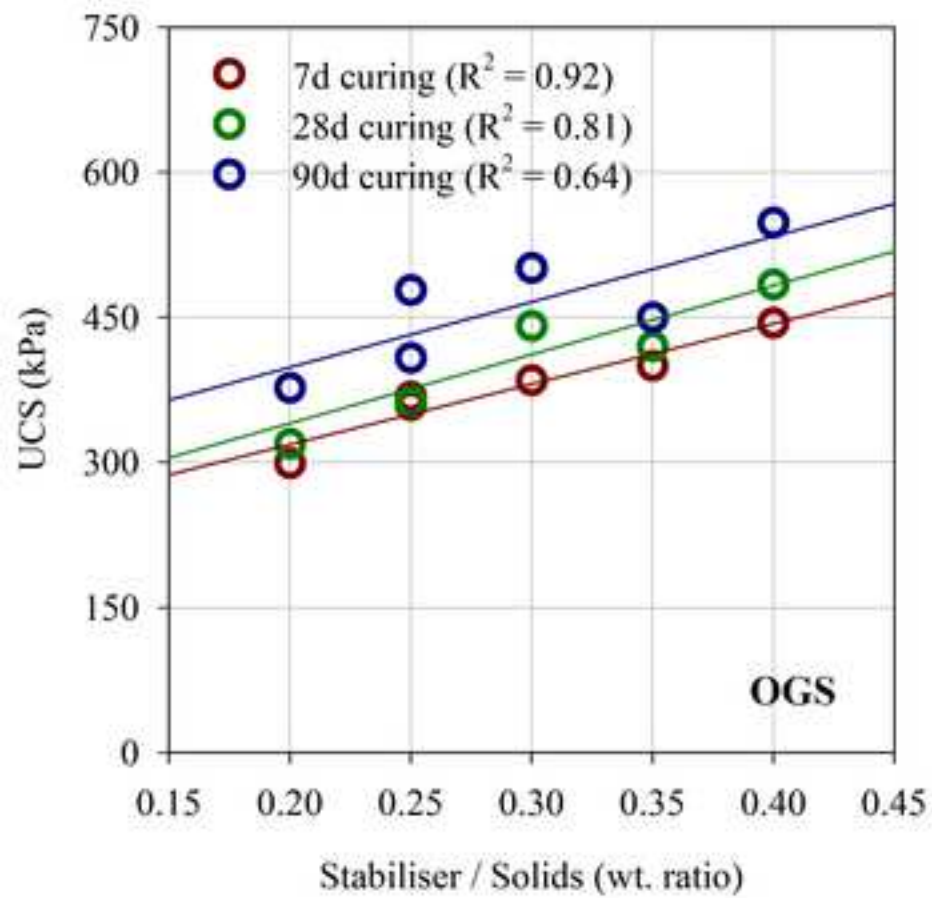












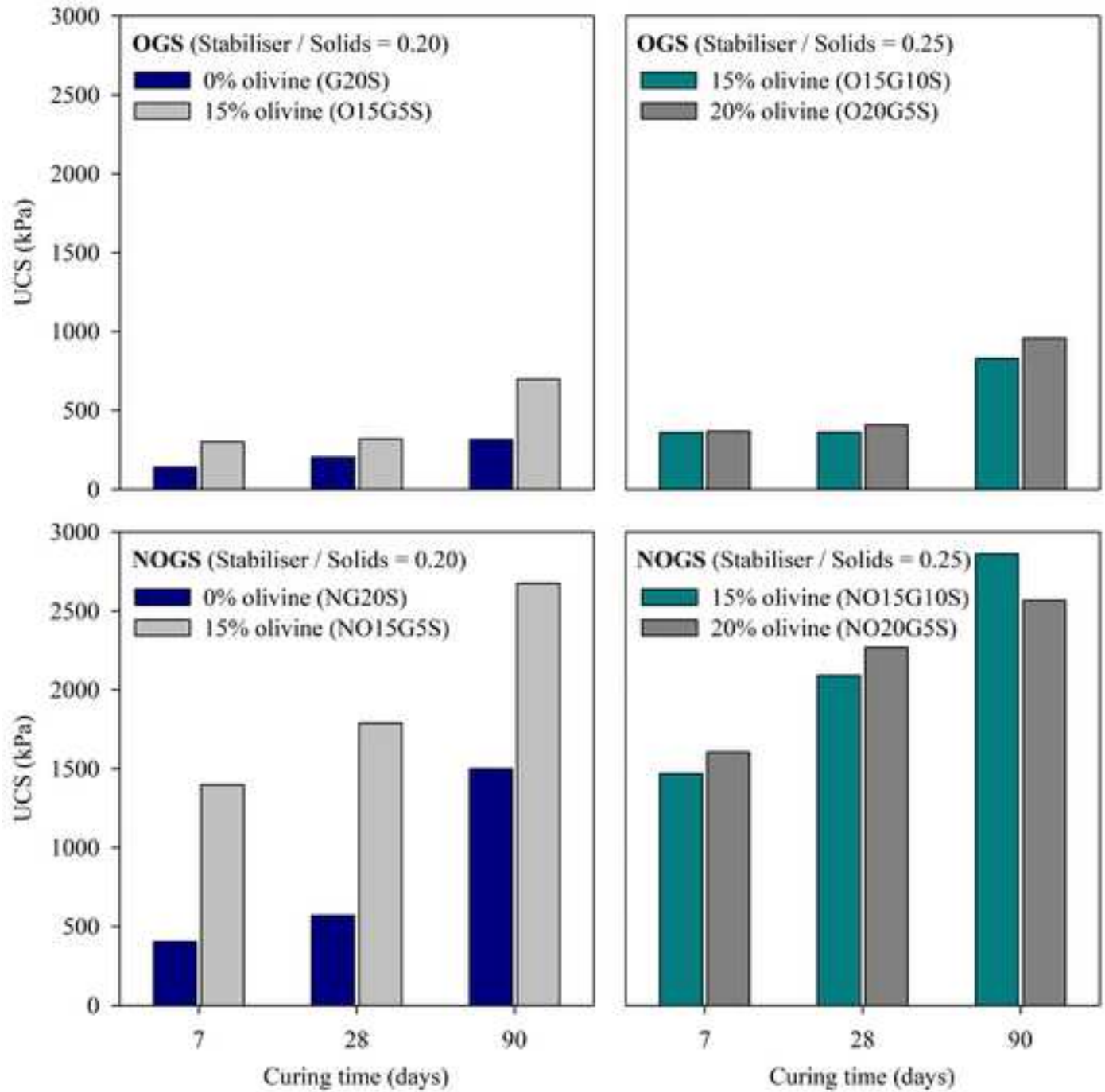


Table 1: Geotechnical characteristics of the clayey soil

Basic soil property	Value	Standard
Specific gravity (Gs)	2.6	BS 1377: Part 2
Liquid limit (%)	60.2	BS 1377: part 2
Plastic limit (%)	30.1	BS 1377: part 2
Optimum water content (%)	32.0	BS 1377: part 4
Maximum dry density (Mg/m ³)	1.3	BS 1377: part 4
Unconfined compressive strength (kPa)	80-100	BS 1377: part 7

Table 2: Chemical composition of the soil, olivine and GGBS

Compound	Soil (%)	Olivine (%)	GGBS (%)
Silica (SiO ₂)	30.98	40.32	34.10
Alumina (Al ₂ O ₃)	18.35	1.37	13.50
Iron oxide (Fe ₂ O ₃)	12.80	8.90	0.36
Calcium oxide (CaO)	0.20	1.13	42.70
Magnesium oxide (MgO)	6.67	48.28	0.20
Loss on ignition	-	9.68	1.40

Table 3: Summary of the mixtures considered

Group	ID	Soil (wt.%)	NaOH (Molar)	GGBS (wt.%)	Olivine (wt.%)	Olivine / GGBS (wt. ratio)	Stabiliser / Solids (wt. ratio) (*)	Water content (wt.%) (**)	Dry density (g/cm ³) (**)
S	S	100	-	-	-	-	-	32.0	1.35
NS	NS	100	10	-	-	-	-	29.0	1.38
GS	G ₅ S	95	-	5	-	-	0.05	31.5	1.36
	G ₁₀ S	90	-	10	-	-	0.10	31.0	1.38
	G ₂₀ S	80	-	20	-	-	0.20	30.0	1.38
OGS	O ₁₅ G ₅ S	80	-	5	15	3.0	0.20	30.0	1.42
	O ₁₅ G ₁₀ S	75	-	10	15	1.5	0.25	27.5	1.54
	O ₁₅ G ₂₀ S	65	-	20	15	0.75	0.35	25.8	1.68
	O ₂₀ G ₅ S	75	-	5	20	4.0	0.25	28.3	1.50
	O ₂₀ G ₁₀ S	70	-	10	20	2.0	0.30	26.0	1.63
	O ₂₀ G ₂₀ S	60	-	20	20	1.0	0.40	23.5	1.84
NGS	NG ₅ S	95	10	5	-	-	0.05	28.5	1.40
	NG ₁₀ S	90	10	10	-	-	0.10	26.0	1.40
	NG ₂₀ S	80	10	20	-	-	0.20	24.0	1.42
NOGS	NO ₁₅ G ₅ S	80	10	5	15	3.0	0.20	28.0	1.55
	NO ₁₅ G ₁₀ S	75	10	10	15	1.5	0.25	26.4	1.67
	NO ₁₅ G ₂₀ S	65	10	20	15	0.75	0.35	24.0	1.75
	NO ₂₀ G ₅ S	75	10	5	20	4.0	0.25	22.3	1.82
	NO ₂₀ G ₁₀ S	70	10	10	20	2.0	0.30	20.0	1.87
	NO ₂₀ G ₂₀ S	60	10	20	20	1.0	0.40	18.3	1.94

(*) 'Stabiliser' and 'Solids' were defined as GGBS + Olivine and Soil + GGBS + Olivine, respectively

(**) Obtained from standard Proctor tests

Table 4: Average atomic ratios for mixtures O₂₀G₂₀S and NO₂₀G₂₀S, after 90 days curing

Ratio	O ₂₀ G ₂₀ S	NO ₂₀ G ₂₀ S
Si/Al	1.38	1.661
Mg/Si	0.031	0.063
Ca/Si	0.124	0.133
Mg/Al	0.046	0.162
Ca/Al	0.182	0.291